The mechanisms for filling carbon nanotubes with molten salts: carbon nanotubes as energy landscape filters

2009 J. Phys.: Condens. Matter 21 115301

(http://iopscience.iop.org/0953-8984/21/11/115301)

J. Phys.: Condens. Matter **21** (2009) 115301 (6pp) doi:10.1088/0953-8984/21/11/115301

The mechanisms for filling carbon nanotubes with molten salts: carbon nanotubes as energy landscape filters

Clare L Bishop[1] **and Mark Wilson**[2]

[1] Department of Chemistry, University College London, 20 Gordon Street, London WC1H 0AJ, UK
[2] Department of Chemistry, Physical and Theoretical Chemistry Laboratory, University of Oxford, South Parks Road, Oxford OX1 3QZ, UK

Received 9 December 2008, in nal form 14 January 2009
Published 19 February 2009
Online at stacks.iop.org/JPhysCM/21/115301

Abstract
The mechanisms for lling carbon nanotubes with molten salts are investigated using molecular dynamics computer simulation. Inorganic nanotubular structures, whose morphologies can be rationalized in terms of the folding, or the removal of sections from, planes of square nets are found to form. The formation mechanisms are found to follow a 'chain-by-chain' motif in which the structures build systematically from charge neutral M–X–M–X· · · chains. The formation mechanisms are rationalized in terms of the ion–ion interactions (intra-chain and inter-chain terms). In addition, the mechanisms of lling are discussed in terms of a 'hopping' between basins on the underlying energy landscape. The role of the carbon nanotube as an energy landscape lter is discussed.

(Some gures in this article are in colour only in the electronic version)

1. Introduction

The discovery of fullerene and nanotubular structures, rstly for carbon [1], but subsequently for a wider range of materials [2], leads to the tantalizing hypothesis that such structures may be ubiquitous. Each nanotubular structure can be considered as as occupying a metastable region of the underlying energy landscape in which these low-dimensional entities are thermodynamically unstable with respect to the (more widely understood) three-dimensional crystal structures. A central question, therefore, becomes how one might access the metastable landscape and hence promote the growth of these tubular structures. Detailed (atomistic) control over the growth of the inorganic nanotubes (INTs) is critical if their potentially useful mechanical and electronic properties are to be fully exploited. An understanding of the atomistic origin of the thermodynamic and kinetic factors which control INT formation is crucial. The encapsulation of the material by the carbon nanotubes disrupts the ionic melt structure and hence modi es the underlying energy landscape. The result of this is that the INT structures may become *global* minima on the landscape with the carbon nanotubes acting as effective *energy landscape filters*. The potential advantage of using carbon nanotubes to template INT growth is that they may allow for a more controlled growth compared with the more extreme physical or chemical conditions often employed [3]. In addition, molten salts represent a useful class of lling materials as their typically low surface tensions fail to crush the carbon tubes on entry. Signi cant experimental progress has been made with a number of salts inserted, including chalcogenides (NiO, Bi_2O_3, V_2O_5, MoO_3, Sb_2O_3, PbO and HgTe [4–11]) and halides (UCl_4 [12], AgCl/AgBr [13, 14], KI [15, 16], BaI_2 [17], CoI_2 [18], metal trihalides [19–21], PbI_2 [22] and $ZrCl_4$ [23]).

In this paper we consider the mechanisms of formation of small diameter INTs within exible carbon nanotubes (C-NTs) in terms of the underlying energy landscapes. Our strategy is to perform physically-motivated modi cations to potential models and hence control the underlying energy landscape both thermodynamically (by controlling the relative basin energy minima) and kinetically (by controlling the energy barriers between basins). Our aim is to uncover the fundamental mechanisms behind the nanotube lling, information on which is dif cult to obtain from experimental observation.

The morphologies of the smallest INTs may be relatively dif cult to understand as the narrow pore C-NTs represent the most extreme con ning environment. Conversely, however, these structures will contain relatively few ions and so their formation mechanisms may be relatively easy to follow and hence understand. In addition, the pseudo-one-dimensional environment may greatly simplify the understanding of the energy landscape. Furthermore, as the carbon pore diameter increases, multi-walled INTs may form, further complicating the understanding of the underlying energy landscape.

2. Background

Previous simulation work has highlighted the existence of two distinct classes of INT, constructed from percolating hexagonal and square nets respectively [24–29]. In both cases the structures of the observed INTs can be rationalized in terms of the folding of the respective hexagonal-and square-net sheets about a given chiral vector [30], $\mathbf{C}_h = (n\mathbf{a}_1 + m\mathbf{a}_2)$, where $\mathbf{a}_1$ and $\mathbf{a}_2$ are the respective unit cell vectors. As a result, the morphologies of the INTs may be expressed in the form $(n, m)_X$, where $X = hex$ or sq de nes whether the tube is formed by folding a hexagonal or square net. The folding of the hexagonal net is the direct analogue of the folding of a graphene sheet to yield a carbon nanotube. These general classi cations incorporate experimental observation. For example, for both KI [31] and AgCl/AgBr [13, 14] the observed crystal structures, interpreted in terms of sections of *bulk* crystal structures, are, in fact, special cases of folded INT structures which also correspond directly to bulk sections [32].

The energetics of the combined carbon and inorganic nanotubes (which sits inside the C-NT) may be mapped onto an analytic model in which the system energy is broken down into terms of the energy required to form the INT from the planar sheet (the folding energy) and the energy of interaction between the INT and the C-NT [25]. In such a simpli ed model the key parameter, which controls the energetics, becomes the difference in C-NT and INT radii.

3. Simulation models

In the present work three potential models are considered, details of which are given elsewhere [30]. The ion–ion interactions are modelled using Born–Mayer effective pair potentials utilizing formal ion (± 1) charges. The three potential models differ in terms of the relative energetics of key bulk crystal structures, in this case the rocksalt (6:6 coordination, B1) and wurtzite (4:4 coordination, B4) structures. The relative energies of these key polymorphs is controlled by varying the short-range interaction parameters (effectively controlling the ion radius ratio). Potential I refers to a model which predicts energy minima for the B4 and B1 polymorphs at equal energies (and different volumes). Potential II refers to the B4 structure being energetically favoured over the B1, whilst potential III refers to the B1 being favoured over the B4. The ion–carbon interactions are accounted for by Lennard-Jones potentials, with the parameters obtained by reference to the noble gas atoms (Ar and Xe respectively) isoelectronic with K^+ and I^-. The carbon–carbon interactions are modelled using a Tersoff-II potential [33] which has been shown to account for both key bulk and C-NT [30] properties. The use of relatively simple models, as opposed to the potentially more accurate electronic structure methods [34], allows for the computationally-tractable study of a wide range of different lling morphologies. Furthermore, it allows the lling process to be directly observed on simulation timescales [24, 35], information which is dif cult to obtain from experimental investigation.

4. Calculations

Two basic strategies are employed in the present work. In the rst case ideal INT structures are constructed from ideal square and hexagonal nets and relaxed to locate the corresponding local energy minima. In the second case, molecular dynamics simulations are performed to model the direct lling of the carbon tubes.

4.1. Static structure energetics

An effective energy landscape for the possible INT structures, as a function of the INT radius (which appears to be the most useful system variable to consider), can be constructed by performing a series of energy minimization calculations in which the radii of a range of INT structures are varied. The hexagonal- or square-net INTs are generated from the respective in nite two-dimensional sheets by folding along the appropriate chiral vector. The local energy minima are identi ed by relaxing these con gurations using a steepest descent algorithm. The simulation cells are periodically repeated with the systems containing between around 100 and 1000 ions, corresponding to cell lengths of the order of 50 A (and corresponding to between one and ten unit cells depending upon the INT morphology).

Figure 1 shows the results of such calculations for potentials II and III. Several key features should be noted. For large radius INTs the energy minima for the square planar and hexagonal sheet INTs tend to their respective in nite plane limits (the energies of the respective in nite two-dimensional hexagonal and square nets). As a result, for potential II the hexagonal INTs appear energetically favourable at relatively large INT radii whilst for potential III the reverse energetic ordering is observed consistent with the relative energies of the underlying bulk rocksalt and wurtzite crystal structures. At small radii the energetic ordering of the respective INT morphologies becomes more complex. The evolution of the energy minima as a function of the INT radius for the hexagonal INTs follows a relatively simple R^{-2} dependence as be ts a continuum elastic model (i.e. those systems behave as macroscopic sheets) [30]. The evolution of the energy with radius for the square-net INTs, however, follows a more complex dependence with the energy minima showing a strong morphology dependence which can be traced back to the speci c ion–ion interactions [30]. The result is that the energies of the $(n, n)_{sq}$ INTs show a different dependence

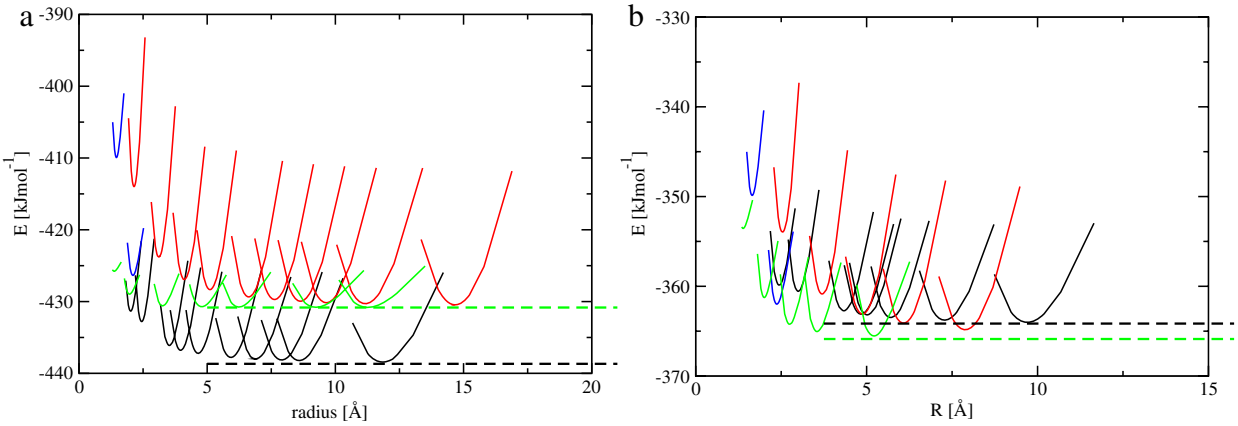

Figure 1. Energy landscapes for potentials (a) II and (b) III as a function of INT radius, R^{INT}. Key: black lines—$(n, m)_{\mathrm{hex}}$, red lines—$(n, 0)_{\mathrm{sq}}$, green lines—$(n, n)_{\mathrm{sq}}$, blue lines—$(n, m)_{\mathrm{sq}}$ $(n \neq m, m \neq 0)$. The dashed lines indicate the limiting energies of the hexagonal—(black) and square planes (green), respectively. (In the print version, (a) lower, upper, low-middle and upper-middle, respectively. (b) Lower-middle, upper, lower and upper-middle, respectively.)

on radius (following an approximate R^{-3} behaviour) than the $(n, 0)_{\mathrm{sq}}$ INTs. INTs of morphology $(n, m)_{\mathrm{sq}}$ $(n \neq m, m \neq 0)$ show an intermediate behaviour.

4.2. Direct filling simulations

To emphasize the subtle thermodynamic and kinetic balance between INTs on the energy landscape a test system, here the (9, 9) C-NT (diameter 12.57 A) with salt modelled using potential I, is lled from multiple liquid con guration starting points. Successive con gurations are generated by performing molecular dynamics on the pure liquid and extracting con gurations at time intervals of the order or ten times the characteristic relaxation time (here of the order of 50 ps as determined from the coherent intermediate scattering functions). For each liquid con guration a charge neutral cylindrical section is removed and the C-NT inserted. The system is then brought back to equilibrium with the C-NT ends closed. Finally, the ends are removed and the C-NT is allowed to ll. Figure 2(a) shows the lling pro les (the time evolution of the number of ions within the C-NT) for the ve lling events. In four of the ve events the nal INT structure corresponds to a $(2, 2)_{\mathrm{sq}}$ INT containing around 15 MX molecules, whilst in the other the nal structure corresponds to a $(3, 2)_{\mathrm{sq}}$ INT containing around 18 MX molecules. Plateau are observed in the lling pro les which correspond to the formation of well-de ned intermediate (highly ordered) structures. The persistence times of these plateaux are signi cant, corresponding to many thousand molecular dynamics steps. In this case the rst intermediate structure formed is a $(1, 1)_{\mathrm{sq}}$ 'ladder', which can be considered as formed from two parallel M–X–M–X$\cdots$ ion chains. The next observed structure is a $(1 \times 3)_{\mathrm{sq}}$ 'hinge' (a molecular graphics 'snapshot' of which is shown in the gure), which can be considered as a 'three-chain' extension of the $(1, 1)_{\mathrm{sq}}$ structure. The 'hinge' structure is unique in the present context as, although it can clearly be constructed from a section of square-net plane, it is not related via a simple folding transformation. For both the $(1, 1)_{\mathrm{sq}}$ and $(1 \times 3)_{\mathrm{sq}}$ structures, with highly anisotropic cross-sections, the exibility of the encasing C-NT, in the form of elliptical distortions, is critical in their stabilization [36]. The dihedral angle of the $(1 \times 3)_{\mathrm{sq}}$ structure of $\sim$100° represents a balance between minimizing the energy of the ionic structure (which would lead to a planar structure, minimizing the like–like electrostatic repulsions between the outer chains) and the energy of interaction between the INT and the C-NT. The exibility of the encasing C-NT is critical in stabilizing these structures with highly anisotropic cross-sections [36].

Figure 2(b) shows a section of the underlying energy landscape for potential I in the presence of the (9, 9) C-NT. The effect of adding the C-NT/INT interaction energy (highlighted in the gure) is to thermodynamically discriminate against larger radii INTs (where the INT structure is pushed against the C-NT inner repulsive wall). The transition between these structures can be understood in terms of thermodynamically-driven 'hopping' between successive energy basins on this landscape. Here the mechanism follows a 'chain-by-chain' motif in which successive (charge neutral) M–X–M–X$\cdots$ chains are added, giving the order $(1, 1)_{\mathrm{sq}} \longrightarrow (1 \times 3)_{\mathrm{sq}} \longrightarrow (2, 2)_{\mathrm{sq}} \rightharpoonup (3, 2)_{\mathrm{sq}}$. Three points are worthy of speci c comment. Firstly, the $(2, 2)_{\mathrm{sq}}$ and $(3, 2)_{\mathrm{sq}}$ minima are close in energy, re ect ing the n e balance between their respective radii and the morphology dependence of the folding energy. As a result, the transformation to the $(3, 2)_{\mathrm{sq}}$ structure, which occurs from the $(2, 2)_{\mathrm{sq}}$ basin, is not strongly thermodynamically driven. To further support the idea of basin 'hopping' at these thermal energies (at 800 K, RT $\sim$ 7 kJ mol^{-1} highlighted in gure 2(b)), we note that a number of 'reverse hops' (transformations in which the number of chains in the INT structure falls) are observed on the simulation timescale. In these cases both the transformations $(1, 1)_{\mathrm{sq}} \longleftrightarrow (1 \times 3)_{\mathrm{sq}}$ and $(1 \times 3)_{\mathrm{sq}} \longleftrightarrow (2, 2)_{\mathrm{sq}}$ are observed. Secondly, the minimum for the $(2, 2)_{\mathrm{hex}}$ INT structure lies at a lower energy then either the corresponding $(2, 2)_{\mathrm{sq}}$ or $(3, 2)_{\mathrm{sq}}$ INT minima. However, a mechanism to transform from a

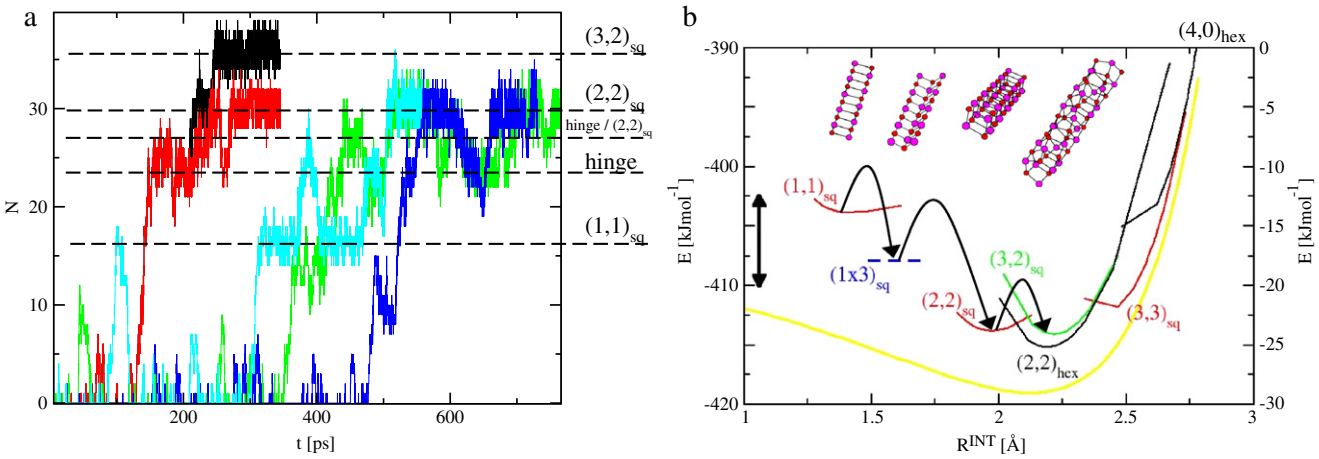

Figure 2. (a) Filling pro les (the number of ions inside the C-NT) as a function of time. The different shaded (coloured online) lines correspond to results from simulations beginning from distinct liquid con gurat ions. The dashed lines highlight the plateaux which correspond to the formation of highly ordered intermediates, the structures of which are indicated to the right of the gure. (b) The energy landscape for potential I modi ed by the presence of the (9, 9) C-NT. The INT morphologies are indicated on the gure and the C-NT/INT interaction energy indicated by the light curve (yellow online). The arrows indicate the 'chain-by-chain' basin hopping mechanism by which the C-NT lls. The energy scale for the INTs is given by the left ordinate, whilst that for the C-NT/INT interaction is given by the right ordinate. The gure inset shows the four structures formed during the lling process. From left to right, the $(1, 1)_{sq}$ 'ladder', $(1 \times 3)_{sq}$ 'hinge', $(2, 2)_{sq}$ and $(3, 2)_{sq}$ containing two, three, four and ve M–X–M–X$\cdots$ chains respectively. The thermal energy at the lling temperature ($T \sim 800$ K) is also indicated by the double arrow.

square planar to a hexagonal structure involves the breaking of bonds which equates to a relatively high activation barrier for this process compared with the 'chain-by-chain' building mechanism to give the $(3, 2)_{sq}$ structure. As a result, the square-plane-based structures appear kinetically stable over hexagonal INTs of similar radii. Thirdly, the effect of the encasing C-NT interaction can be seen for the larger radii INTs on this landscape. As a result, the $(3, 3)_{sq}$ INT becomes inaccessible on the simulation timescales as, although only marginally thermodynamically unfavourable with respect to the $(3, 2)_{sq}$ INT, the insertion of a sixth ion chain involves too high an activation barrier to be accessed.

Figure 3 shows a section of the energy landscape for the lling of the (9, 9) C-NT using potential II. The inset to the gure shows the lling pro le which displays a clear plateau from $t \sim 115$ to $\sim$150 ps ($\cong$60 000 MD steps) which again corresponds to the formation of a well-de ned highly ordered intermediate crystal structure. The formation mechanism again follows a 'chain-by-chain' pattern, here $(1, 1)_{sq} \longrightarrow (1 \times 3)_{sq}$. Although both the $(2, 2)_{sq}$ and $(2, 2)_{hex}$ structures appear thermodynamically stable with respect to the $(1 \times 3)_{sq}$, the activation barrier to the formation of these structures is suf ciently high so as to preclude their formation on the simulation timescale. In particular, the $(1 \times 3)_{sq} \longrightarrow (2, 2)_{sq}$ 'transition', which features the addition of a fourth ion chain, is precluded by the elliptical deformation of the C-NT cross-section imposed by the formation of the highly anisotropic $(1 \times 3)_{sq}$ structure. The C-NT deforms such that the major axis of the elliptical cross-section correlates with the widest section of the inorganic 'hinge'.

Figure 4 shows a section of the energy landscape for potential III and the (9, 9) C-NT. Again, the lling pro le (not shown) shows a number of plateaux indicative of relatively

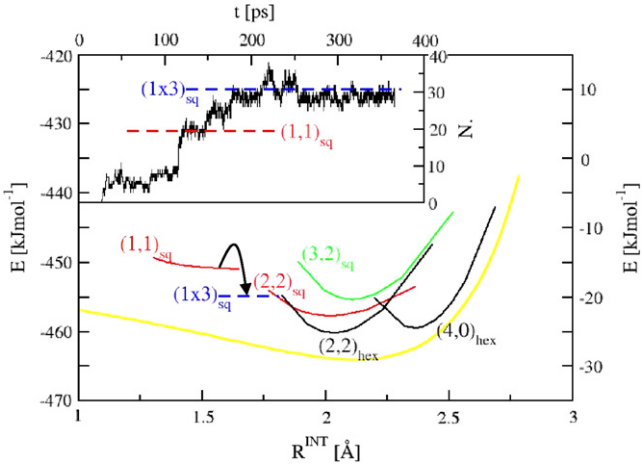

Figure 3. The energy landscape for potential II modi ed by the presence of the (9, 9) C-NT. The key is as for gure 2.

stable intermediate structures leading to the nal $(3, 3)_{sq}$ INT structure. The mechanism of formation in this case shows subtle differences to the previous two, following the pattern $(1, 1)_{sq} \longrightarrow (2, 2)_{sq} \longrightarrow (2, 2)_{hex} \longrightarrow (3, 2)_{sq} \longrightarrow (3, 3)_{sq}$. The lack of a clear $(1 \times 3)_{sq}$ intermediate structure is the result of the $(1, 1)_{sq} \longrightarrow (2, 2)_{sq}$ transformation occurring via a 'folding/unfolding' mechanism (previously observed in the lling of xed carbon tubes [32]) in which MX molecules, whose 'bonds' are aligned perpendicular to the C-NT major axis, move along the [110] direction (hence forming the characteristic $(2, 2)_{sq}$ cubes from the $(1, 1)_{sq}$ squares). Furthermore, a $(2, 2)_{sq} \longrightarrow (2, 2)_{hex}$ is observed. Both of these observations can be attributed to the greater space in the C-NT afforded by this potential, which favours the bulk

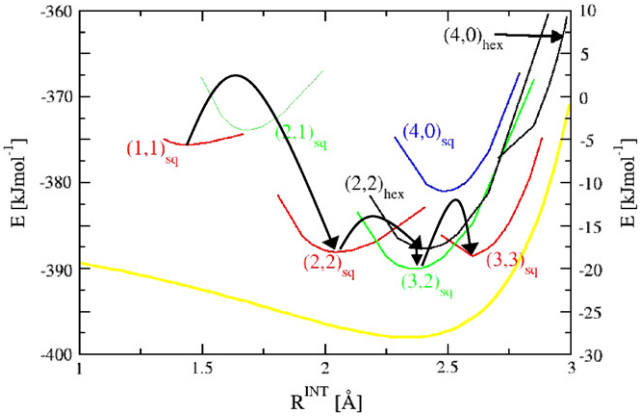

Figure 4. The energy landscape for potential III modi ed by the presence of the (9, 9) C-NT. The key is as for gure 2.

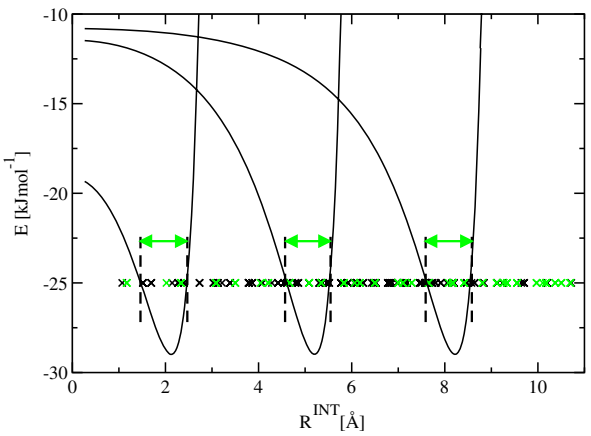

Figure 5. Schematic representation of how the C-NTs act as energy landscape lters. The crosses indicate ideal radii for the square-net (light crosses/green online) and hexagonal-net (dark crosses/black online) INTs. The curves show (from left to right) the C-NT/INT interactions with C-NT diameters of 12, 18 and 24 A respectively. In each case the interactions act to favour the formation of the range of INT radii indicated.

B1 structure and hence more tightly packed clusters than either potentials I or II. On formation of the initial $(1, 1)_{sq}$ 'ladder' suf cient space is available so as to promote the 'folding/unfolding' mechanism (which is equivalent to adding a further $(1, 1)_{sq}$ structure in one go). In addition, there is enough free volume to allow the $(2, 2)_{sq} \longrightarrow (2, 2)_{hex}$ transformation which promotes an alternative pathway to the $(3, 2)_{sq}$ structure before the n al chain insertion to give the $(3, 3)_{sq}$ INT.

5. Discussion

Figure 5 shows a schematic diagram to explain the action of the C-NTs as energy landscape lters in determining the INT structure formed from a given ionic melt. The nite number of folding chiral vectors for a given two-dimensional sheet effectively 'quantizes' the landscape in terms of the accessible INT radii (highlighted by the crosses in the gure for both square- and hexagonal-net-based INTs). The presence of the C-NTs provide an energy well which acts to thermodynamically stabilize a range of INT radii, the location of which depends critically on the C-NT radius (three examples of which are shown in the gure). As a result, the C-NTs can be considered as thermodynamically ltering speci c INTs from the overall landscape.

The linking theme of the observed lling events is the 'hopping' between energy basins promoted at the thermal energies afforded above typical salt melting temperatures. The atomistic process associated with these hops is the addition (or removal) of a M–X–M–X $\cdots$ chain. Bichoutskaia and Pyper [37] have decomposed the energetics of pseudo-one-dimensional bulk (rocksalt) structures into contributions from intra- and inter-chain interactions. We have recently extended this work to help explain the relative energetics of the high symmetry $(n, 0)_{sq}$ and $(n, n)_{sq}$ INTs as a function of their radii [30]. The key result in the present context is that the inter-chain contribution appears smaller than the intra-chain energy. As a result, the sort of motion observed dynamically in the present work, in which a single ion chain moves across a building ionic cluster, appears relatively energetically facile.

A key factor in explaining this facility is to note that, although the individual ions possess formal valence charges, the motion of the ion chains in this concerted fashion corresponds to the motion of charge neutral species. As a result, the activation energies for the ion motion are signi cantly smaller for the chains than would be the case for the motion of a single ion as the relatively large energies required to break nearest-neighbour counter-ion bonds are near-counter-balanced by the presence of additional counter ions in the chain.

Overall, therefore, the chain-by-chain construction of the INTs is essentially thermodynamically driven with the thermodynamic driving force provided by the presence of the encasing C-NT. However, the charge neutrality of the M–X–M–X$\cdots$ chains means that relatively small thermodynamic driving forces may promote INT growth. In addition, the C-NTs may distort away from the ideal circular cross-section in order to adopt the more anisotropic INT structures. Again, the energy required to distort the C-NT is counter-balanced by the INT formation energy.

It is important to note that the existence of each INT with a corresponding local energy minima on the energy landscape indicates these structures to be (meta)stable in the absence of the con ning INT. The C-NT provides the thermodynamic driving force for the INT formation in the form of an energy well (of the sort indicated in gure 5). Removal of the con ning carbon tube removes this local energy well but the local energy minima (i.e. of the form observed in gure 1) for the formed INT remains. Overall, therefore, the result of removing the C-NT is to effectively open up the underlying phase diagram, translating the INT structure from a true thermodynamically stable state to a metastable state (with respect to the bulk crystal structures). Further molecular dynamics simulations indicate that these INT structures are typically stable to temperatures of the order of the bulk crystal melting points. Such observations are, of course, unsurprising given the metastability of the C-NTs themselves

as well as other experimentally-obtained INT structures. The generic metastability of these INT structures can, therefore, be ascribed to the relatively high activation barriers associated with their potential transformations to the thermodynamic bulk crystal structure ground states. However, in certain cases the symmetry of a given INT may allow for a relatively low (or zero) energy transformation to an alternative INT structure (as observed here for transformations between square- and hexagonal-based nets).

6. Summary

In summary, the mechanism by which a small diameter carbon nanotube lls from molten salts has been investigated. The underlying energy landscapes have been controlled by modifying the ionic potential models in a systematic way. The observed mechanisms, which are dominated by a 'chain-by-chain' building up process, are consistent with the relatively low energetics associated with such motions. The linking theme is that the carbon nanotubes behave as energy landscape lters in the sense that they not only stabilize metastable regions on the phase diagrams (which contain the low-dimensional INT crystal structures) but also stabilize speci c ranges of INT radii. The use of a exible representation of the con ning carbon tube appears crucial in promoting these mechanisms.

References

[1] Kroto H W, Heath J R, O'Brien S C, Curl R F and Smalley R E 1985 *Nature* **318** 162–3
[2] Bar-Sadan M, Kaplan-Ashiri I and Tenne R 2007 *Eur. Phys. J. Special Top.* **149** 71–101
[3] Tenne R, Homyonfer M and Feldman Y 1998 *Chem. Mater.* **10** 3225
[4] Tsang S C, Chen Y K, Harris P J F and Green M L H 1994 *Nature* **372** 159–62
[5] Ajayan P M, Ebbesen T W, Ichihashi T, Iijima S, Tanigaki K and Hiura H 1993 *Nature* **362** 522–5
[6] Ajayan P M, Ichihashi T and Iijima S 1993 *Chem. Phys. Lett.* **202** 384–8
[7] Ajayan P M, Stephan O, Redlich Ph and Colliex C 1995 *Nature* **375** 564–7
[8] Chen Y K, Green M L H and Tsang S C 1996 *Chem. Commun.* 2489–90
[9] Friedrichs S, Meyer R R, Sloan J, Kirkland A I, Hutchison J L and Green M L H 2001 *Chem. Commun.* 929–30
[10] Hulman M, Kuzmany H, Costa P M F J, Friedrichs S and Green M L H 2004 *Appl. Phys. Lett.* **85** 2068
[11] Carter R, Sloan J, Kirkland A I, Meyer R R, Lindan P J D, Lin G, Green M L H, Vlandas A, Hutchison J L and Harding J H 2006 *Phys. Rev. Lett.* **96** 215501
[12] Sloan J, Cook J, Chu A, Zwiefka-Sibley M, Green M L H and Hutchison J L 1998 *J. Solid State Chem.* **140** 83–90
[13] Sloan J, Wright D M, Woo H-G, Bailey S R, Brown G, York A P E, Coleman K S, Hutchison J L and Green M L H 1999 *Chem. Commun.* 699–700
[14] Sloan J, Terrones M, Nufer S, Friedrichs S, Bailey S R, Woo H-G, Rühle M, Hutchison J L and Green M L H 2002 *J. Am. Chem. Soc.* **124** 2116–7
[15] Sloan J, Novotny M C, Bailey S R, Brown G, Xu C, Williams V C, Friedrichs S, Flahaut E, Callendar R L, York A P E, Coleman K S, Green M L H, Dunin-Borkowski R E and Hutchison J L 2000 *Chem. Phys. Lett.* **329** 61–5
[16] Meyer R R, Sloan J, Dunin-Borkowski R E, Kirkland A I, Novotny M C, Bailey S R, Hutchison J L and Green M L H 2000 *Science* **289** 1324–6
[17] Sloan J, Grosvenor S J, Friedrichs S, Kirkland A I, Hutchison J L and Green M L H 2002 *Angew Chem. Int. Edn* **41** 1156
[18] Philp E, Sloan J, Kirkland A I, Meyer R R, Friedrichs S, Hutchison J L and Green M L H 2003 *Nat. Mater.* **2** 788–91
[19] Friedrichs S, Kirkland A I, Meyer R R, Sloan J and Green M L H 2004 *Electron Microsc. Anal.* p 455
[20] Friedrichs S and Green M L H 2005 *Z. Metallk.* **96** 419
[21] Friedrichs S, Falke U and Green M L H 2005 *ChemPhysChem* **6** 300
[22] Flahaut E, Sloan J, Friedrichs S, Kirkland A I, Coleman K S, Williams V C, Hanson N, Hutchison J L and Green M L H 2006 *Chem. Mater.* **18** 2059
[23] Brown G, Bailey S R, Sloan J, Xu C, Friedrichs S, Flahaut E, Coleman K S, Green M L H, Hutchison J L and Dunin-Borkowski R E 2001 *Chem. Commun.* 845
[24] Wilson M and Madden P A 2001 *J. Am. Chem. Soc.* **123** 2101
[25] Wilson M 2002 *J. Chem. Phys.* **116** 3027
[26] Wilson M 2002 *Chem. Phys. Lett.* **366** 504–9
[27] Wilson M 2004 *Nano Lett.* **4** 299–302
[28] Wilson M 2004 *Chem. Phys. Lett.* **397** 340
[29] Wilson M 2006 *J. Chem. Phys.* **124** 124706
[30] Bishop C L and Wilson M 2008 *Mol. Phys.* **106** 1665–74
[31] Meyer R R, Sloan J, Dunin-Borkowski R E, Kirkland A I, Novotny M C, Bailey S R, Hutchison J L and Green M L H 2000 *Science* **289** 1324–6
[32] Wilson M 2007 *J. Chem. Soc. Faraday Trans.* **134** 283
[33] Tersoff J 1988 *Phys. Rev.* B **37** 6991
[34] Sceats E L, Green J C and Reich S 2006 *Phys. Rev.* B **73** 125441
[35] Baldoni M, Leoni S, Sgamellotti A, Seifert G and Mercuri F 2007 *Small* **3** 1730
[36] Bishop C L and Wilson M 2009 *J. Mater. Chem.* at press
[37] Bichoutskaia E and Pyper N C 2006 *J. Phys. Chem.* B **110** 5936